

Resolvin D1 limits 5-lipoxygenase nuclear localization and leukotriene B₄ synthesis by inhibiting a calcium-activated kinase pathway

Gabrielle Fredman^{a,1}, Lale Ozcan^a, Stefano Spolitu^a, Jason Hellmann^b, Matthew Spite^b, Johannes Backs^c, and Ira Tabas^{a,1}

^aDepartment of Medicine, Department of Pathology and Cell Biology, and Department of Physiology, Columbia University, New York, NY 10032; ^bInstitute of Molecular Cardiology, University of Louisville, Louisville, KY 40202; and ^cLaboratory for Cardiac Epigenetics, Department of Cardiology, Heidelberg University, and German Centre for Cardiovascular Research (DZHK), 69120 Heidelberg, Germany

Edited by Mauro Perretti, Queen Mary University of London, London, United Kingdom, and accepted by the Editorial Board August 26, 2014 (received for review June 13, 2014)

Imbalances between proinflammatory and proresolving mediators can lead to chronic inflammatory diseases. The balance of arachidonic acid-derived mediators in leukocytes is thought to be achieved through intracellular localization of 5-lipoxygenase (5-LOX): nuclear 5-LOX favors the biosynthesis of proinflammatory leukotriene B₄ (LTB₄), whereas, in theory, cytoplasmic 5-LOX could favor the biosynthesis of proresolving lipoxin A₄ (LXA₄). This balance is shifted in favor of LXA₄ by resolvin D1 (RvD1), a specialized proresolving mediator derived from docosahexaenoic acid, but the mechanism is not known. Here we report a new pathway through which RvD1 promotes nuclear exclusion of 5-LOX and thereby suppresses LTB₄ and enhances LXA₄ in macrophages. RvD1, by activating its receptor formyl peptide receptor2/lipoxin A₄ receptor, suppresses cytosolic calcium and decreases activation of the calcium-sensitive kinase calcium-calmodulin-dependent protein kinase II (CaMKII). CaMKII inhibition suppresses activation P38 and mitogen-activated protein kinase-activated protein kinase 2 kinases, which reduces Ser271 phosphorylation of 5-LOX and shifts 5-LOX from the nucleus to the cytoplasm. As such, RvD1's ability to decrease nuclear 5-LOX and the LTB₄:LXA₄ ratio in vitro and in vivo was mimicked by macrophages lacking CaMKII or expressing S271A-5-LOX. These findings provide mechanistic insight into how a specialized proresolving mediator from the docosahexaenoic acid pathway shifts the balance toward resolution in the arachidonic acid pathway. Knowledge of this mechanism may provide new strategies for promoting inflammation resolution in chronic inflammatory diseases.

Persistent inflammation and its failed resolution underlie the pathophysiology of prevalent human diseases, including cancer, diabetes, and atherosclerosis (1). Hence, uncovering mechanisms to suppress inflammation and enhance resolution is of immense interest (2–5). Resolution is orchestrated in part by specialized proresolving mediators (SPMs), including lipoxins, resolvins, protectins, and maresins (2), and by protein and peptide mediators (6). A common protective function of SPMs is their ability to limit excessive proinflammatory leukotriene formation without being immunosuppressive (2, 7). Specifically, resolvin D1 (RvD1) is protective in several disease models (8) and limits excessive leukotriene B₄ (LTB₄) production without compromising host defense (7, 9). However, the mechanism underlying these actions of RvD1 is not well understood.

Arachidonic acid (AA) is first converted into 5-hydroperoxyeicosatetraenoic acid (5-HPETE) and then into leukotriene A₄ (LTA₄) by 5-lipoxygenase (5-LOX) (10, 11). Subsequent hydrolysis of LTA₄ by LTA₄ hydrolase yields LTB₄ (10, 11). During inflammation, 5-LOX is phosphorylated and translocates to the nuclear membrane, which favors the biosynthesis of LTB₄ (12–17). However, major gaps remain in our understanding of the relevance of this pathway to primary cells and animal models and how they are regulated by SPMs. Further, it is currently not known how this pathway may influence the biosynthesis of lipoxin A₄ (LXA₄), which is a SPM that also requires 5-LOX. These gaps are

critical because although LTB₄ is crucial for host defense, exuberant production underlies the basis for several inflammatory diseases and impairs endogenous resolution programs (11, 18). Moreover, complete blockade of LTB₄ biosynthetic enzymes may compromise host defense; thus, understanding new mechanisms that temper LTB₄ production is essential for translational research in this area (19).

Here, we report that RvD1, by suppressing the activation of the calcium-sensing kinase calcium-calmodulin-dependent protein kinase II (CaMKII), decreases the phosphorylation and nuclear localization of 5-LOX and thereby limits LTB₄ biosynthesis. These results provide a mechanistic understanding of how RvD1 tempers proinflammatory responses to facilitate a rapid transition to resolution.

Results

RvD1 Suppresses AA-Stimulated LTB₄ by Blocking P38/MK2-Mediated 5-LOX Phosphorylation and Nuclear Localization. We first showed that 1 nM RvD1 enhanced AA-stimulated LXA₄ generation (Fig. 1A) and blocked LTB₄ formation in both bone marrow-derived macrophages and zymosan-elicited peritoneal macrophages (Fig. 1B and *SI Appendix, Fig. S1 and S2A*). We conducted an RvD1 dose–response experiment and found that the suppression of AA-stimulated LTB₄ generation was close to maximal at 1 nM RvD1

Significance

Specialized proresolving mediators, such as resolvin D1 (RvD1), are endogenous molecules that both dampen inflammation without compromising host defense and promote tissue resolution. A prime example is RvD1's ability to decrease the ratio of proinflammatory leukotriene B₄ (LTB₄) to proresolving lipoxin A₄ (LXA₄), but the mechanism is not known. We have discovered a new calcium kinase signaling pathway through which RvD1 lowers the nuclear:cytoplasmic ratio of 5-lipoxygenase (5-LOX), the common enzyme for LTB₄ and LXA₄ biosynthesis. This shift in 5-LOX localization dampens LTB₄ production and enhances LXA₄ production. By providing a new mechanistic understanding of how RvD1 tempers inflammation to facilitate resolution, these findings can help devise new therapeutic strategies for diseases driven by nonresolving inflammation.

Author contributions: G.F., L.O., and I.T. designed research; G.F., S.S., J.H., and M.S. performed research; J.B. and I.T. contributed new reagents/analytic tools; G.F., S.S., J.H., M.S., and I.T. analyzed data; and G.F., L.O., and I.T. wrote the paper.

The authors declare no conflict of interest.

This article is a PNAS Direct Submission. M.P. is a Guest Editor invited by the Editorial Board.

Freely available online through the PNAS open access option.

¹To whom correspondence may be addressed. Email: iat1@columbia.edu or gf2269@columbia.edu.

This article contains supporting information online at www.pnas.org/lookup/suppl/doi:10.1073/pnas.1410851111/-DCSupplemental.

macrophages with DYKDDDDK (FLAG)-tagged plasmids encoding either wild-type or S271A 5-LOX. Similar transfection efficiency for the two vectors was confirmed by anti-FLAG FACS (*SI Appendix, Fig. S6*). We found that S271A 5-LOX mimicked the ability of RvD1 to suppress nuclear 5-LOX and LTB₄ in AA-treated macrophages, and the effects of RvD1 and the mutant were non-additive (*Fig. 3 B and C*). These data, along with the previously known role of nuclear 5-LOX in LTB₄ biosynthesis (17), suggest that RvD1 limits LTB₄ synthesis by blocking AA-stimulated P38-MK2 activation and the subsequent phosphorylation and nuclear localization of 5-LOX.

RvD1 Limits the P38/MK2/Nuclear 5-LOX/LTB₄ Pathway by Suppressing AA-Induced CaMKII Activation. AA has been shown to rapidly increase intracellular calcium (Ca²⁺) (28), which prompted us to investigate whether a calcium-signaling protein might play a role in this pathway. We were particularly interested in CaMKII because CaMKII has been shown to activate P38 and MK2 in other settings (29, 30). Stimulation of macrophages with AA led to an increase in phospho-CaMKII, the enzyme's active form, and phospho-CaMKII was decreased by RvD1 in a FPR2/ALX-dependent manner (*Fig. 4A*). The FPR2/ALX ligand LXA₄ also blocked AA-stimulated phospho-CaMKII and phospho-MK2 (*SI Appendix, Fig. S7*). As a possible mechanism for suppression of CaMKII activation, we found that RvD1 suppressed the rise in cytosolic calcium that occurs with AA treatment of macrophages (*SI Appendix, Fig. S8 A and C*).

To show causation related to CaMKII, we studied macrophages from *Camk2g^{fl/fl}LysMCre^{+/-}* mice, which lack the macrophage isoform, CaMKII γ (*SI Appendix, Fig. S9*). The increase in

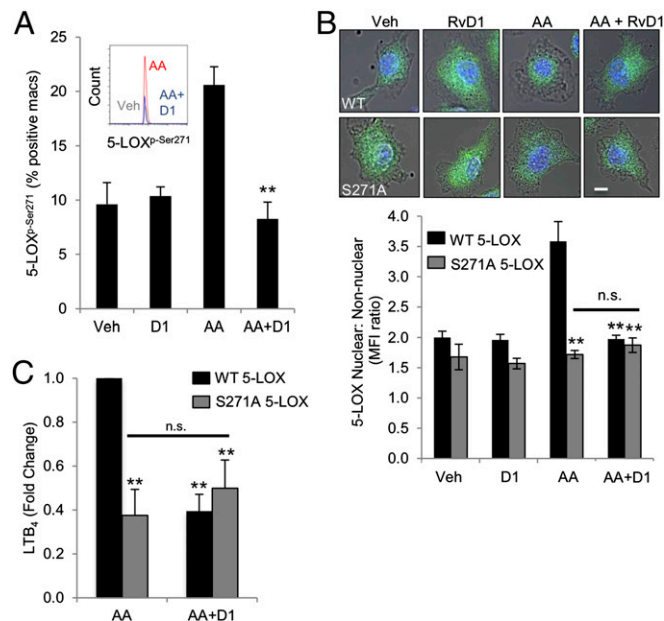


Fig. 3. AA-induced nuclear 5-LOX and LTB₄ is suppressed in macrophages expressing S271A-5-LOX. BMDMs incubated as in *Fig. 1A*. (A) Flow cytometric analysis for anti-phospho-Ser²⁷¹-5-LOX fluorescence ($n = 3$; mean \pm SEM; $*P < 0.05$ versus AA). (B and C) BMDMs were transfected with FLAG-tagged wild-type 5-LOX or S271A 5-LOX for 72 h before incubations. In B, the cells were then permeabilized and stained with Alexa-488 anti-Flag antibody (green), counterstained with the nuclear stain DAPI (blue), and viewed by confocal microscopy at 40 \times magnification. Representative cells, with the fluorescence image superimposed on the phase-contrast images and quantification of mean fluorescence intensity of nuclear versus nonnuclear FLAG staining of 5–7 cells per field are shown. (Scale bar = 5 μ m.) In C, LTB₄ was assayed by ELISA and expressed relative to the value for AA alone. For B and C, $n = 3$, mean \pm SEM; $**P < 0.05$ versus AA/wild-type; n.s., nonsignificant.

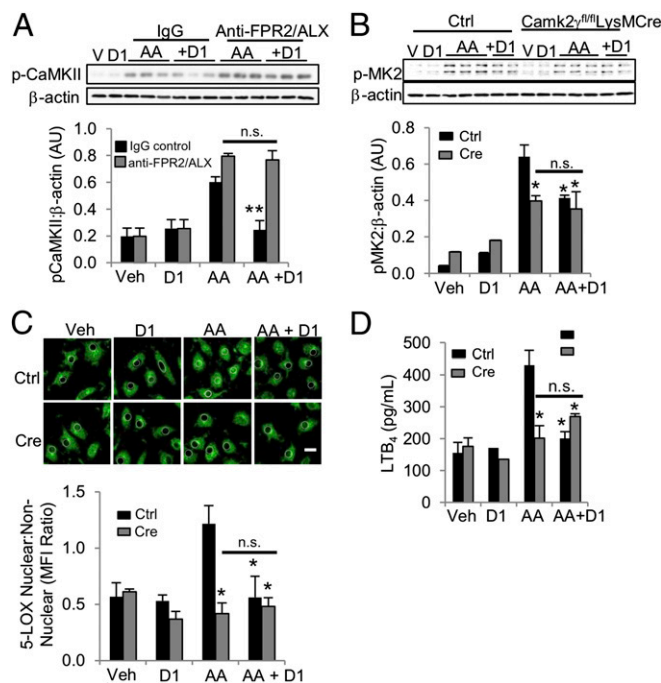


Fig. 4. RvD1 suppresses the p38-MK2-LTB₄ pathway by inhibiting CaMKII. (A) BMDMs were treated as in *Fig. 1A*, except IgG control or blocking anti-ALX/FPR2 IgG were included; V, vehicle control. Cell extracts were immunoblotted for p-CaMKII and β -actin loading control and quantified by densitometry ($n = 3$, mean \pm SEM; $*P < 0.05$ versus AA). (B) BMDMs from control (*Camk2g^{fl/fl}*) mice or *Camk2g^{fl/fl}LysMCre^{+/-}* mice were incubated as in A (without blocking antibody), immunoblotted for p-MK2 and β -actin, and quantified by densitometry. (C) 5-LOX nuclear versus nonnuclear localization was assayed as in *Fig. 2C*. (Scale bar = 10 μ m.) (D) LTB₄ was assessed by ELISA. For B–D, $n = 3$, mean \pm SEM; $**P < 0.05$ versus AA-control; n.s., nonsignificant.

phospho-MK2 by AA was significantly decreased in CaMKII-deficient macrophages compared with control *Camk2g^{fl/fl}* macrophages, indicating that CaMKII was upstream of MK2. Moreover, RvD1's ability to limit phosphorylation of MK2 was abolished in CaMKII-deficient macrophages, suggesting that RvD1 acts in the same pathway as CaMKII (*Fig. 4B*). Most important, AA-stimulated 5-LOX nuclear localization and LTB₄ production were decreased in macrophages lacking CaMKII, and the suppressive actions of RvD1 and CaMKII deficiency were not additive (*Fig. 4 C and D*). These data support the premise that RvD1 signals through CaMKII to limit LTB₄ production.

To further prove causation, we transduced macrophages with an adenovirus expressing constitutively active T287D CaMKII (CA-CaMKII), which mimics autophosphorylation and is thus autonomously activated in the absence of bound calcium (31). Adenoviral transfection itself did not alter the pathway, as RvD1 blocked AA-stimulated MK2 phosphorylation in adeno-LacZ control cells to a similar degree as in nontransduced wild-type macrophages (*SI Appendix, Fig. S10A* and earlier). In contrast to the situation with wild-type macrophages, RvD1 was unable to block AA-stimulated MK2 activation, 5-LOX nuclear localization, and LTB₄ production in CA-CaMKII-transduced macrophages (*SI Appendix, Fig. S10A–C*), suggesting that RvD1 acts by blocking CaMKII activation.

RvD1 also blocked AA-stimulated phospho-MK2 and LTB₄ generation in human monocyte-derived macrophages, and this effect was dependent on both FPR2/ALX and an RvD1 receptor unique to human cells, GPR32 (*SI Appendix, Fig. S11 A–C*). Moreover, human macrophages transduced with dominant negative K43A CaMKII (31) exhibited diminished AA-stimulated LTB₄

generation that was not further decreased by RvD1 (*SI Appendix, Fig. S11D*). These data suggest similar pathways of RvD1-mediated LTB₄ suppression in mouse and human macrophages.

The RvD1-CaMKII-p38-MK2 Pathway Is Functional in Vivo. To examine whether the RvD1-LTB₄ signaling pathway is operable in vivo, we used a model of acute zymosan-induced peritoneal inflammation in which controlled release of LTB₄ by resident macrophages in the early stages of inflammation is a critical determinant for swift resolution (18). As predicted, RvD1 treatment decreased zymosan-induced LTB₄ generation (*SI Appendix, Fig. S12C*) and polymorphonuclear neutrophil (PMN) infiltration (*SI Appendix, Fig. S12D*) (9). Most important, these events were accompanied by a decrease in phospho-p38 (*SI Appendix, Fig. S12A*) and phospho-MK2 (*SI Appendix, Fig. S12B*) in exudate macrophages.

We then compared these responses in *Camk2g^{fl/fl}LysMCre^{+/-}* versus *Camk2g^{fl/fl}* mice and found that macrophage-CaMKII deficiency led to decreases in both zymosan-stimulated LTB₄ and PMN infiltration in a manner that was not additive with RvD1 (Fig. 5*A–C*). Note that 5-LOX protein levels were not different between the two groups of mice (*SI Appendix, Fig. S13*). To investigate whether the suppression of LTB₄ and PMNs by RvD1 was through phosphorylation of 5-LOX at Ser271 in vivo, we injected *Alox5^{-/-}* mice with plasmids encoding wild-type 5-LOX or S271A 5-LOX. Flow cytometry verified successful transfection of peritoneal macrophages (*SI Appendix, Fig. S14*). We found that S271A 5-LOX-transfected mice exhibited significantly reduced LTB₄ generation and PMN infiltration and that this decrease was not additive with RvD1 (Fig. 5*D and E*). These combined data

demonstrate that RvD1 limits excessive LTB₄ production in vivo by suppressing CaMKII activation and 5-LOX phosphorylation.

Discussion

An important process in inflammation resolution is the dampening of proinflammatory molecules in a manner that does not compromise host defense (2). Thus, it is essential to understand at a molecular-cellular level how this critical process is achieved. We provide here a new pathway (*SI Appendix, Fig. S15*) that applies to a previously recognized example of SPM-mediated inflammation suppression; namely, the ability of RvD1 to decrease LTB₄ levels (9). Moreover, we show here that RvD1 increases the level of LXA₄, which is consistent with the hypothesis that intracellular 5-LOX localization affects the balance of LTB₄ and LXA₄. In this context, the most likely scenario is that LXA₄ is released and then acts in a paracrine and autocrine manner via FPR2/ALX.

Our results indicate that the target of RvD1 in AA-treated macrophages is a new CaMKII pathway that promotes p38-MK2 activation and LTB₄ production. RvD1 suppressed CaMKII activation, most likely by blocking calcium entry into the cytosol, as RvD1 blocked the increment in cytosolic calcium effected by AA, ATP, and fMet-Leu-Phe (*SI Appendix, Fig. S6*). In this regard, RvD1 was recently reported to block histamine-stimulated intracellular calcium in goblet cells in a receptor-dependent manner (32), and the SPM resolvin E1 was shown to block intracellular calcium initiated by the antimicrobial peptide LLGDFFRKSKEKIGKEFKRIVQRIKDFLRNLPVPTES (LL-37) in PMNs (33). Interestingly, another study showed that LL-37 stimulated p38 and LTB₄ formation in PMNs (34), although the signal transduction pathway leading to p38 activation was not elucidated. These findings, together with the data herein, suggest that the ability of SPMs to rapidly and transiently limit intracellular calcium and CaMKII-p38-MK2 signaling may be a fundamental mechanism for preventing excessive or prolonged inflammation (33, 35).

CaMKII has been shown to mediate other cellular processes in diseases in which chronic inflammation is important, raising the possibility of additional beneficial effects of RvD1. For example, CaMKII triggers endoplasmic reticulum-stress-induced apoptosis in macrophages (36), which could be important in diseases in which leukocyte apoptosis and secondary necrosis underlie the pathology, such as advanced atherosclerosis and certain autoimmune diseases (37, 38). Moreover, in the setting of obesity, CaMKII promotes excessive hepatic glucose production and impairs hepatic insulin signaling by activating a p38-MK2-mediated pathway (29, 30). Although the action of RvD1 in hepatocytes remains to be explored, RvD1 has been shown to promote insulin sensitivity in diabetic mice, in part by enhancing insulin signaling (39).

In humans, the ratio of proresolving LXA₄ to proinflammatory LTB₄ is balanced when inflammation is properly controlled (7, 18), whereas this balance is skewed toward LTB₄ in certain chronic inflammatory diseases (40–42). Although the mechanisms of excess LTB₄ production in these diseases remain to be elucidated, it is possible that defective RvD1 levels or activity play a role through the mechanisms elucidated in this report. For example, atherosclerosis, a disease characterized by failed inflammation resolution (43), is associated with excessive production of LTB₄ (11), and 5-LOX has been shown to be located in the nuclear region of macrophages in human atherosclerotic lesions (44).

In summary, our results provide a mechanistic understanding of how RvD1 carries out one of its most important proresolving functions; namely, suppressing LTB₄ production while boosting LXA₄ synthesis. The new pathway elucidated in this report suggests that therapeutic administration of RvD1 and possibly other SPMs may be particularly beneficial for inflammatory diseases in

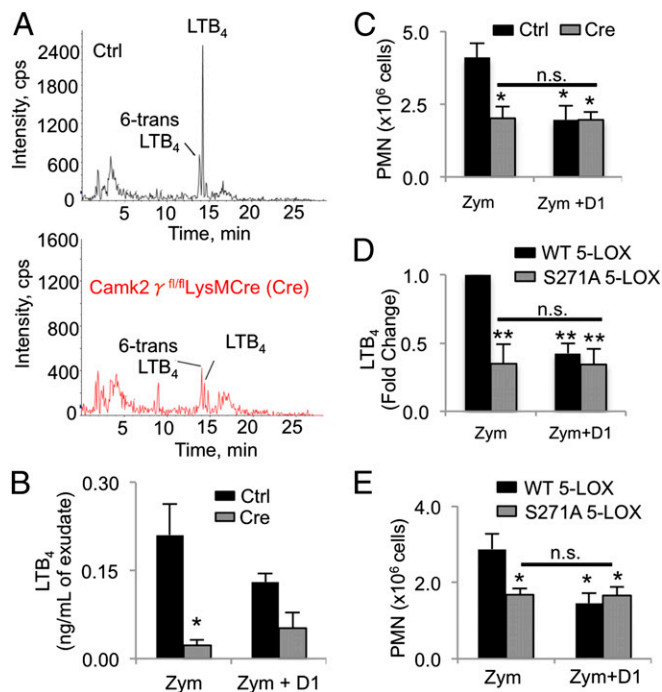


Fig. 5. Evidence for the RvD1–CaMKII–p5-LOX pathway in vivo. (A) Representative chromatograms of LTB₄ and 6-trans-LTB₄ (335 > 195) in inflammatory exudates of control (Ctrl), *Camk2g^{fl/fl}* (Ctrl), or *Camk2g^{fl/fl}LysMCre^{+/-}* mice 2 h after i.p. zymosan. (B and C) Quantification of LTB₄ and PMNs in inflammatory exudates of the indicated groups of mice treated with zymosan in the presence or absence of 10 ng i.v. RvD1 (for LTB₄). (D and E) *Alox5^{-/-}* mice were transfected with plasmids encoding wild-type or S271A 5-LOX 42 h before sequential RvD1 and zymosan treatments and assayed for LTB₄ and PMNs. For B, $n = 3–5$ /group, mean \pm SEM; * $P < 0.05$ versus both control groups; for C–E, $n = 5$ mice/group, mean \pm SEM; * $P < 0.05$ or ** $P < 0.01$ versus Zym/wild-type; n.s., nonsignificant; WT, wild-type.

which excessive CaMKII-p38-MK2 activation or LTB₄ underlies the pathology.

Materials and Methods

LTB₄ Detection in Vitro. Bone marrow-derived macrophages (BMDMs) were harvested from female C57BL/6J mice (6–8 wk of age) and cultured in DMEM, 10% (vol/vol) FBS, 20% (vol/vol) L cell media containing macrophage colony stimulating factor, glutamine, and penicillin/streptomycin for 7 d. For individual experiments, 3×10^6 macrophages in 300 μ L PBS containing calcium and magnesium were incubated with 1 nM RvD1 for 20 min at 37 °C (45), followed by AA (10 μ M) or LTA₄ (10 μ M) stimulation. After 40 min, the cells were placed on ice and the media were subjected to ELISA analysis. For FPR2/ALX receptor experiments, IgG or anti-FPR2 (10 μ g/incubation, 37 °C, 1 h) was added before RvD1 stimulation.

Confocal Microscopy for Intracellular Localization of 5-LOX. BMDMs were plated on 8-well coverslips (LabTek) and incubated under various conditions, as described in the figure legends. After addition of 5% cold formalin, BMDMs were incubated for 60 min at 4 °C with permeabilization buffer (cat. no. 554715, BD Biosciences) containing anti-5-LOX antibody. Excess antibody was then removed, and the cells were incubated with Alexa 488 anti-rabbit-IgG for an additional 30 min at 4 °C. The cells were counterstained with Hoechst to identify nuclei, viewed on a Nikon A1 confocal microscope, and analyzed using ImageJ software.

Zymosan A-Stimulated Peritonitis. Six- to 8-wk-old female mice were administered 10 ng RvD1 per mouse by i.v. injection. After 15 min, 200 μ g zymosan A per mouse was injected i.p. to induce peritonitis for 2 h, as in ref. 9. All procedures were conducted in accordance with the Columbia University Standing Committee on Animals guidelines for animal care (protocol no. AC-AAAF7107).

- Nathan C, Ding A (2010) Nonresolving inflammation. *Cell* 140(6):871–882.
- Serhan CN (2010) Novel lipid mediators and resolution mechanisms in acute inflammation: To resolve or not? *Am J Pathol* 177(4):1576–1591.
- Ryan A, Godson C (2010) Lipoxins: Regulators of resolution. *Curr Opin Pharmacol* 10(2):166–172.
- Tabas I, Glass CK (2013) Anti-inflammatory therapy in chronic disease: Challenges and opportunities. *Science* 339(6116):166–172.
- Godson C, Perretti M (2013) Novel pathways in the yin-yang of immunomodulation. *Curr Opin Pharmacol* 13(4):543–546.
- Ortega-Gómez A, Perretti M, Soehnlein O (2013) Resolution of inflammation: An integrated view. *EMBO Mol Med* 5(5):661–674.
- Chiang N, et al. (2012) Infection regulates pro-resolving mediators that lower antibiotic requirements. *Nature* 484(7395):524–528.
- Fredman G, Serhan CN (2011) Specialized proresolving mediator targets for RvE1 and RvD1 in peripheral blood and mechanisms of resolution. *Biochem J* 437(2):185–197.
- Norling LV, Dalli J, Flower RJ, Serhan CN, Perretti M (2012) Resolvin D1 Limits Polymorphonuclear Leukocytes Recruitment to Inflammatory Loci: Receptor-Dependent Actions. *Arterioscler Thromb Vasc Biol* 32(8):1970–8.
- Samuelsson B, Dahlén SE, Lindgren JA, Rouzer CA, Serhan CN (1987) Leukotrienes and lipoxins: Structures, biosynthesis, and biological effects. *Science* 237(4819):1171–1176.
- Haeggström JZ, Funk CD (2011) Lipoxygenase and leukotriene pathways: Biochemistry, biology, and roles in disease. *Chem Rev* 111(10):5866–5898.
- Rouzer CA, Samuelsson B (1987) Reversible, calcium-dependent membrane association of human leukocyte 5-lipoxygenase. *Proc Natl Acad Sci USA* 84(21):7393–7397.
- Rouzer CA, Kargman S (1988) Translocation of 5-lipoxygenase to the membrane in human leukocytes challenged with ionophore A23187. *J Biol Chem* 263(22):10980–10988.
- Wong A, et al. (1991) Influx of extracellular calcium is required for the membrane translocation of 5-lipoxygenase and leukotriene synthesis. *Biochemistry* 30(38):9346–9354.
- Coffey M, Peters-Golden M, Fantone JC, 3rd, Sporn PH (1992) Membrane association of active 5-lipoxygenase in resting cells. Evidence for novel regulation of the enzyme in the rat alveolar macrophage. *J Biol Chem* 267(1):570–576.
- Woods JW, et al. (1993) 5-lipoxygenase and 5-lipoxygenase-activating protein are localized in the nuclear envelope of activated human leukocytes. *J Exp Med* 178(6):1935–1946.
- Serhan CN, Haeggström JZ, Leslie CC (1996) Lipid mediator networks in cell signaling: Update and impact of cytokines. *FASEB J* 10(10):1147–1158.
- Fredman G, Li Y, Dalli J, Chiang N, Serhan CN (2012) Self-limited versus delayed resolution of acute inflammation: Temporal regulation of pro-resolving mediators and microRNA. *Sci Rep* 2:639.
- Di Gennaro A, Haeggström JZ (2014) Targeting leukotriene B4 in inflammation. *Expert Opin Ther Targets* 18(1):79–93.
- Krishnamoorthy S, et al. (2010) Resolvin D1 binds human phagocytes with evidence for proresolving receptors. *Proc Natl Acad Sci USA* 107(4):1660–1665.
- Fiore S, Maddox JF, Perez HD, Serhan CN (1994) Identification of a human cDNA encoding a functional high affinity lipoxin A4 receptor. *J Exp Med* 180(1):253–260.

In Vivo Transfection. Plasmids (10 μ g) were incubated with 16 mL Jet-Pei-Man in vivo transfection reagent (PolyPlus Transfection; cat. no. 203–10G) for at least 30 min at room temperature. These transfection complexes (1 mL) were injected i.p. into 6–8-w-old female *Alox5^{-/-}* mice (Jackson Laboratories). After 42 h, peritonitis experiments were conducted.

Identification and Quantification of Eicosanoids by Liquid Chromatography-MS/MS. Lipid mediators of interest were profiled using an HPLC system (Shimadzu Prominence) equipped with a reverse-phase (C18) column (4.6 \times 50 mm; 5.0 μ m particle size) coupled to a triple quadrupole mass spectrometer (AB Sciex API2000), which was operated in negative ionization mode. Multiple reaction monitoring was used to identify and quantify LTB₄ (335 > 195), 6-*trans*-LTB₄ (335 > 195), and LXA₄ (351 > 115) (46). (For detailed methods see *SI Appendix, Methods*.)

Statistical Analysis. Results are presented as means \pm SEM. Differences between two groups were compared by paired Student *t* test or one-way ANOVA after normality testing. *P* < 0.05 was considered significant.

ACKNOWLEDGMENTS. The authors thank Dr. Eric Olson (University of Texas Southwestern Medical Center) for providing the *Camk2g^{fl/fl}* mice, Theresa Swayne (Columbia University) for assistance with microscopy experiments, and Dr. Harold A. Singer (Albany Medical College) for adeno-T287D-CaMKII and adeno-K43A-CaMKII. This work was supported in part by the National Institutes of Health (NIH) Pathway to Independence K99 Grant HL119587 (to G.F.); NIH/National Heart, Lung, and Blood Institute Program of Excellence in Nanotechnology Award, Contract HHSN268201000045C/BAA-HV-10-08 (to I.T.); NIH/NHLBI R01 HL107497 and HL075662 (to I.T.); NIH Grants HL106173 (to M.S.) and HL116186 (to J.H.); Deutsche Forschungsgemeinschaft BA 2258/2-1 (to J.B.); the European Commission FP7-Health-2010; MEDIA-261409 (to J.B.); Deutsches Zentrum für Herz-Kreislauf-Forschung-German Centre for Cardiovascular Research (J.B.); and BMBF German Ministry of Education and Research (J.B.).

- Cooray SN, et al. (2013) Ligand-specific conformational change of the G-protein-coupled receptor ALX/FPR2 determines proresolving functional responses. *Proc Natl Acad Sci USA* 110(45):18232–18237.
- Wertz O, Szellas D, Steinhilber D, Rådmark O (2002) Arachidonic acid promotes phosphorylation of 5-lipoxygenase at Ser-271 by MAPK-activated protein kinase 2 (MK2). *J Biol Chem* 277(17):14793–14800.
- Luo M, Jones SM, Peters-Golden M, Brock TG (2003) Nuclear localization of 5-lipoxygenase as a determinant of leukotriene B4 synthetic capacity. *Proc Natl Acad Sci USA* 100(21):12165–12170.
- Rådmark O, Wertz O, Steinhilber D, Samuelsson B (2007) 5-Lipoxygenase: Regulation of expression and enzyme activity. *Trends Biochem Sci* 32(7):332–341.
- Godson C, et al. (2000) Cutting edge: Lipoxins rapidly stimulate nonphagocytic phagocytosis of apoptotic neutrophils by monocyte-derived macrophages. *J Immunol* 164(4):1663–1667.
- Maderna P, et al. (2002) Lipoxins induce actin reorganization in monocytes and macrophages but not in neutrophils: Differential involvement of rho GTPases. *Am J Pathol* 160(6):2275–2283.
- Thompson JL, Shuttleworth TJ (2013) Molecular basis of activation of the arachidonate-regulated Ca²⁺ (ARC) channel, a store-independent Orai channel, by plasma membrane STIM1. *J Physiol* 591(Pt 14):3507–3523.
- Ozcan L, et al. (2012) Calcium signaling through CaMKII regulates hepatic glucose production in fasting and obesity. *Cell Metab* 15(5):739–751.
- Ozcan L, et al. (2013) Activation of calcium/calmodulin-dependent protein kinase II in obesity mediates suppression of hepatic insulin signaling. *Cell Metab* 18(6):803–815.
- Pfleiderer PJ, Lu KK, Crow MT, Keller RS, Singer HA (2004) Modulation of vascular smooth muscle cell migration by calcium/calmodulin-dependent protein kinase II-delta 2. *Am J Physiol Cell Physiol* 286(6):C1238–C1245.
- Li D, et al. (2013) Resolvin D1 and aspirin-triggered resolvin D1 regulate histamine-stimulated conjunctival goblet cell secretion. *Mucosal Immunol* 6(6):1119–1130.
- Wan M, Godson C, Guiry PJ, Agerberth B, Haeggström JZ (2011) Leukotriene B4/antimicrobial peptide LL-37 proinflammatory circuits are mediated by BLT1 and FPR2/ALX and are counterregulated by lipoxin A4 and resolvin E1. *FASEB J* 25(5):1697–1705.
- Wan M, Sabirsh A, Wetterholm A, Agerberth B, Haeggström JZ (2007) Leukotriene B4 triggers release of the cathelicidin LL-37 from human neutrophils: Novel lipid-peptide interactions in innate immune responses. *FASEB J* 21(11):2897–2905.
- Ohira T, et al. (2004) A stable aspirin-triggered lipoxin A4 analog blocks phosphorylation of leukocyte-specific protein 1 in human neutrophils. *J Immunol* 173(3):2091–2098.
- Timmins JM, et al. (2009) Calcium/calmodulin-dependent protein kinase II links ER stress with Fas and mitochondrial apoptosis pathways. *J Clin Invest* 119(10):2925–2941.
- Tabas I (2010) The role of endoplasmic reticulum stress in the progression of atherosclerosis. *Circ Res* 107(7):839–850.
- Fredman G, Ozcan L, Tabas I (2014) Common Therapeutic Targets in Cardiometabolic Disease. *Sci Transl Med* 6(239):239ps235.
- Hellmann J, Tang Y, Kosuri M, Bhatnagar A, Spite M (2011) Resolvin D1 decreases adipose tissue macrophage accumulation and improves insulin sensitivity in obese-diabetic mice. *FASEB J* 25(7):2399–2407.

40. Karp CL, et al. (2004) Defective lipoxin-mediated anti-inflammatory activity in the cystic fibrosis airway. *Nat Immunol* 5(4):388–392.
41. Levy BD, et al.; Severe Asthma Research Program, National Heart, Lung, and Blood Institute (2005) Diminished lipoxin biosynthesis in severe asthma. *Am J Respir Crit Care Med* 172(7):824–830.
42. Fredman G, et al. (2011) Impaired phagocytosis in localized aggressive periodontitis: Rescue by Resolvin E1. *PLoS ONE* 6(9):e24422.
43. Tabas I (2010) Macrophage death and defective inflammation resolution in atherosclerosis. *Nat Rev Immunol* 10(1):36–46.
44. Spanbroek R, et al. (2003) Expanding expression of the 5-lipoxygenase pathway within the arterial wall during human atherogenesis. *Proc Natl Acad Sci USA* 100(3): 1238–1243.
45. Dalli J, Serhan CN (2012) Specific lipid mediator signatures of human phagocytes: Microparticles stimulate macrophage efferocytosis and pro-resolving mediators. *Blood* 120(15):e60–e72.
46. Yang R, Chiang N, Oh SF, Serhan CN. Metabolomics-lipidomics of eicosanoids and docosanoids generated by phagocytes. *Curr Protoc Immunol*. 2011;chapter 14: Unit 14.26.

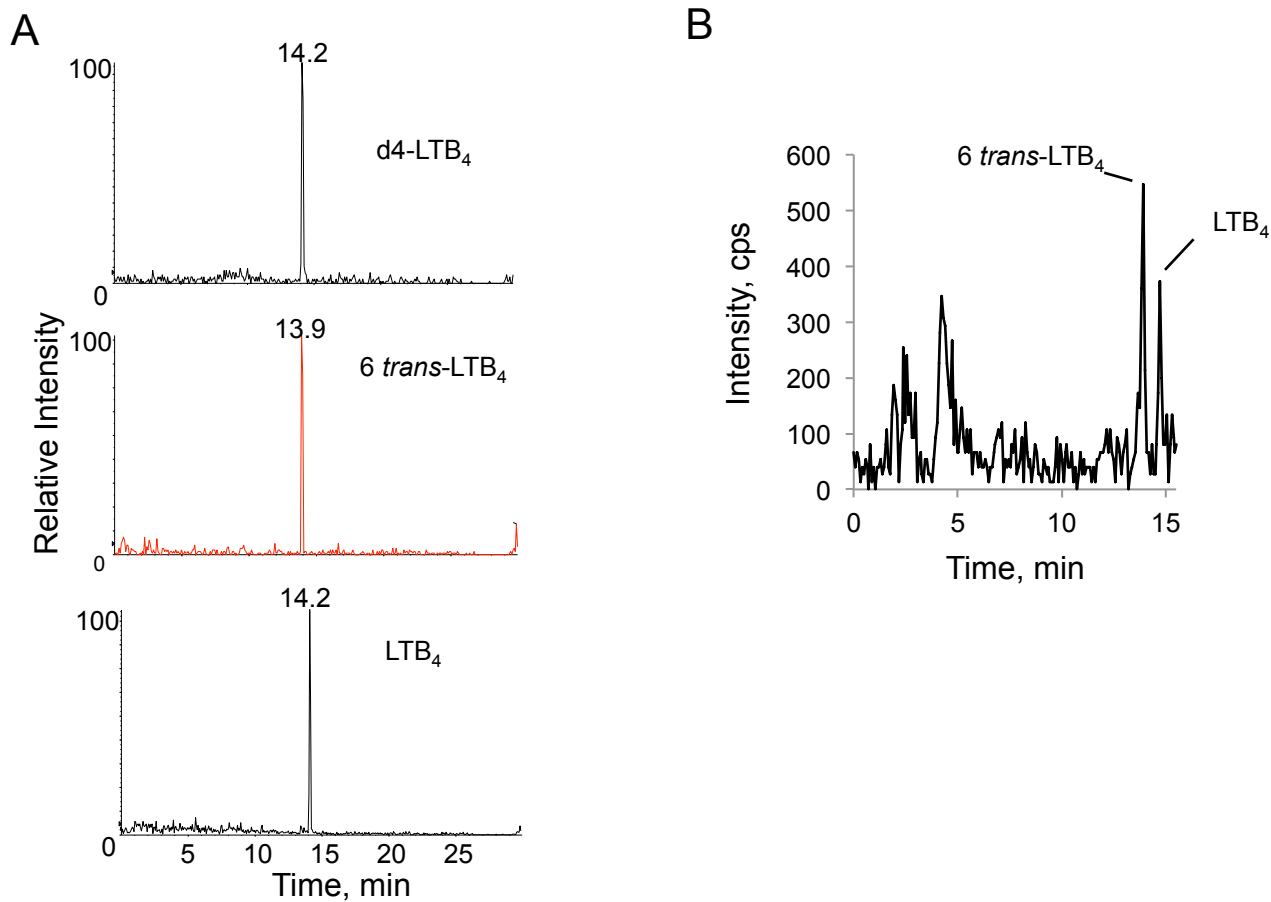


Figure S1. Confirmation of LTB₄ identify in BMDMs. (A) Representative MRM chromatograms of authentic standards of *d4*-LTB₄ (339>197), 6-*trans*-LTB₄, and LTB₄ (335>195), with retention times indicated. (B) Representative MRM chromatogram of LTB₄ and 6-*trans*-LTB₄ (335>195) in BMDMs stimulated with AA.

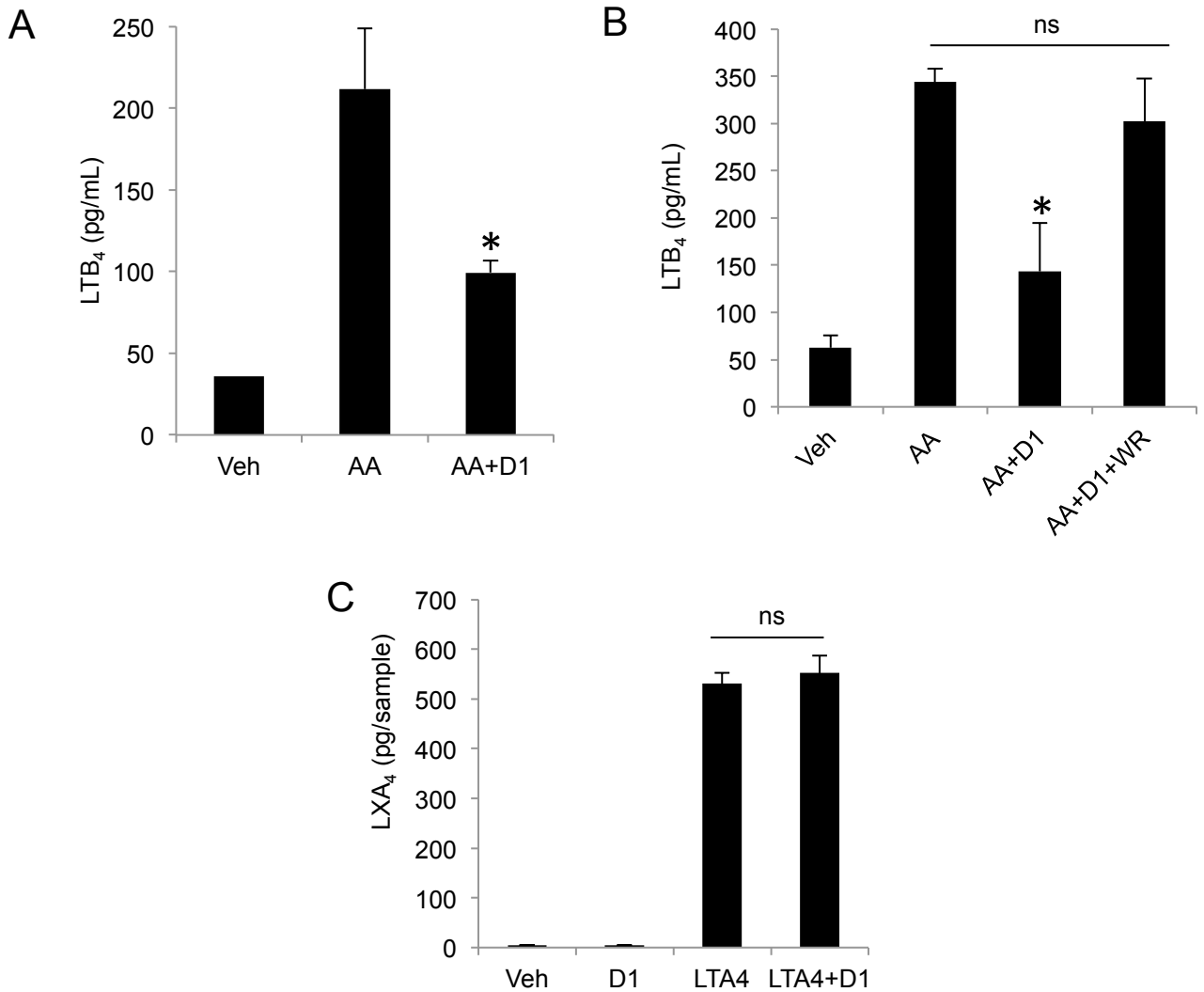


Fig. S2. RvD1 suppresses AA-stimulated LTB₄ in elicited macrophages, requires FPR2/ALX, and enhances LXA₄ upstream of LTA₄ hydrolase. (A) Peritoneal macrophages were harvested from mice 72 h post i.p. zymosan and then incubated and assayed for LTB₄ as in Fig. 1B ($n = 3$; mean \pm SEM; * $P < 0.05$ vs. AA). (B) BMDMs were pre-treated the FPR2/ALX antagonist WRW4 (10 μ M) for 20 min at 37°C and then incubated and assayed for LTB₄ as above ($n = 3$; mean \pm SEM; * $P < 0.05$ vs. AA and AA+D1+WR; n.s., non-significant). (C) BMDMs were incubated with 10 μ M LTA₄ instead of AA as in Fig. 1F, and LXA₄ in the media was assayed ($n = 3$; n.s., non-significant). NB: In this experiment, a PLA₂ inhibitor was included in all incubations ensure that LXA₄ production was being driven by LTA₄ rather than by AA released from cellular phospholipids.

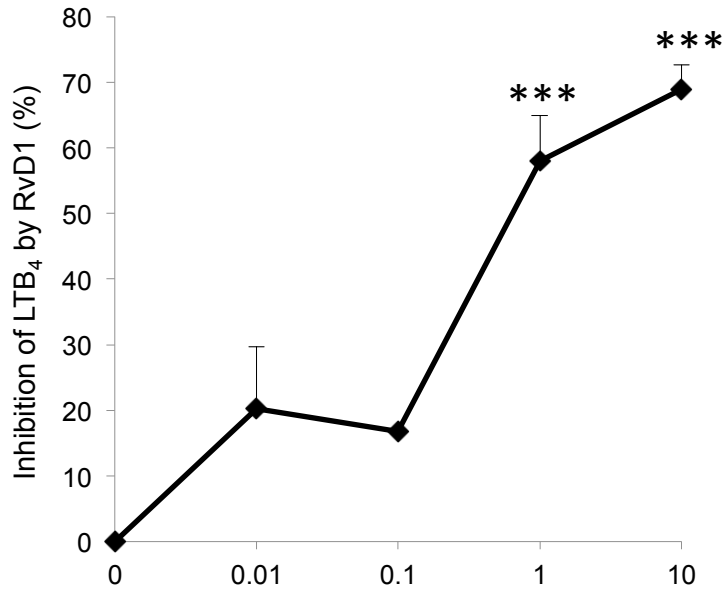


Fig. S3. RvD1 blocks AA-stimulated LTB₄ in a dose-dependent manner. BMDMs were preincubated with vehicle control, 0.01, 0.1, 1 or 10 nM RvD1 15 min, followed by incubation with 10 mM AA for 40 min. The media were then assayed LTB₄ by ELISA ($n = 3$ for ELISA; mean \pm SEM; *** $P < 0.001$ vs. AA).

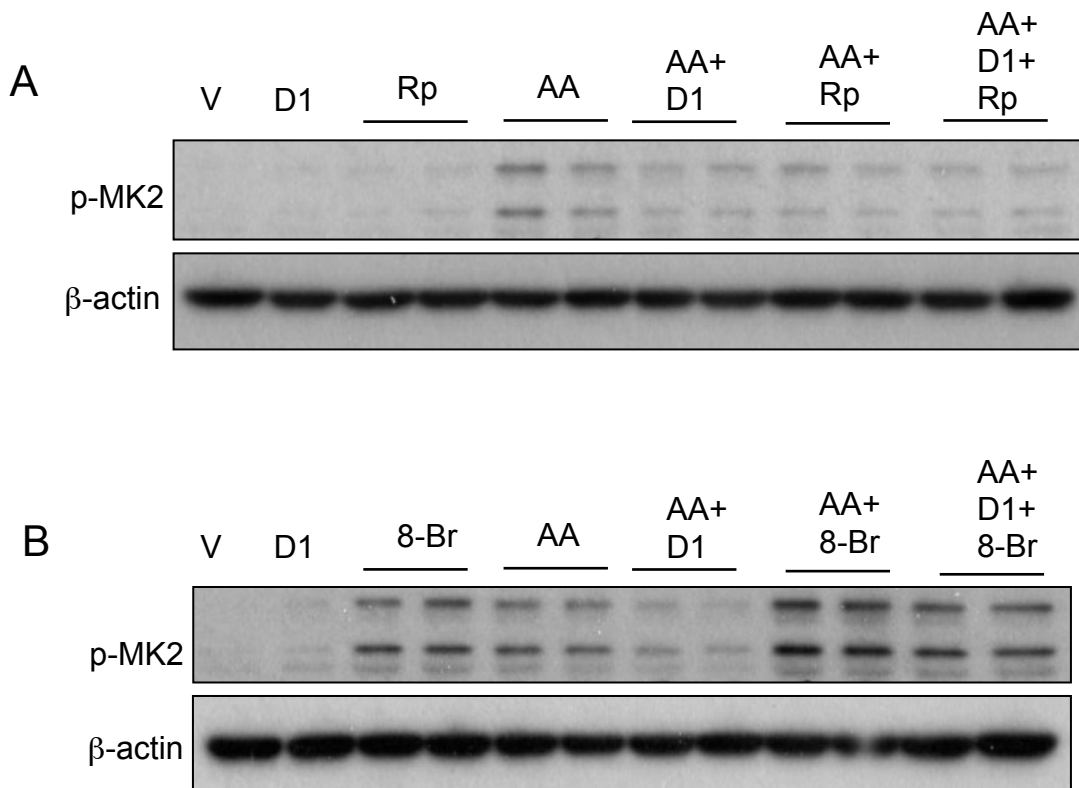


Fig. S4. Suppression of MK2 phosphorylation by RvD1 is mimicked by Rp-cAMP and blocked by 8-bromo-cAMP. (A-B) BMDMs were preincubated for 15 mins with vehicle control (V), RvD1 (D1), Rp-cAMP (Rp), 8-bromo-cAMP (8-Br), or the indicated combinations. The cells were then incubated for 5 min with 10 μ M AA. Cell lysates were immunoblotted for phospho-MK2 and β -actin.

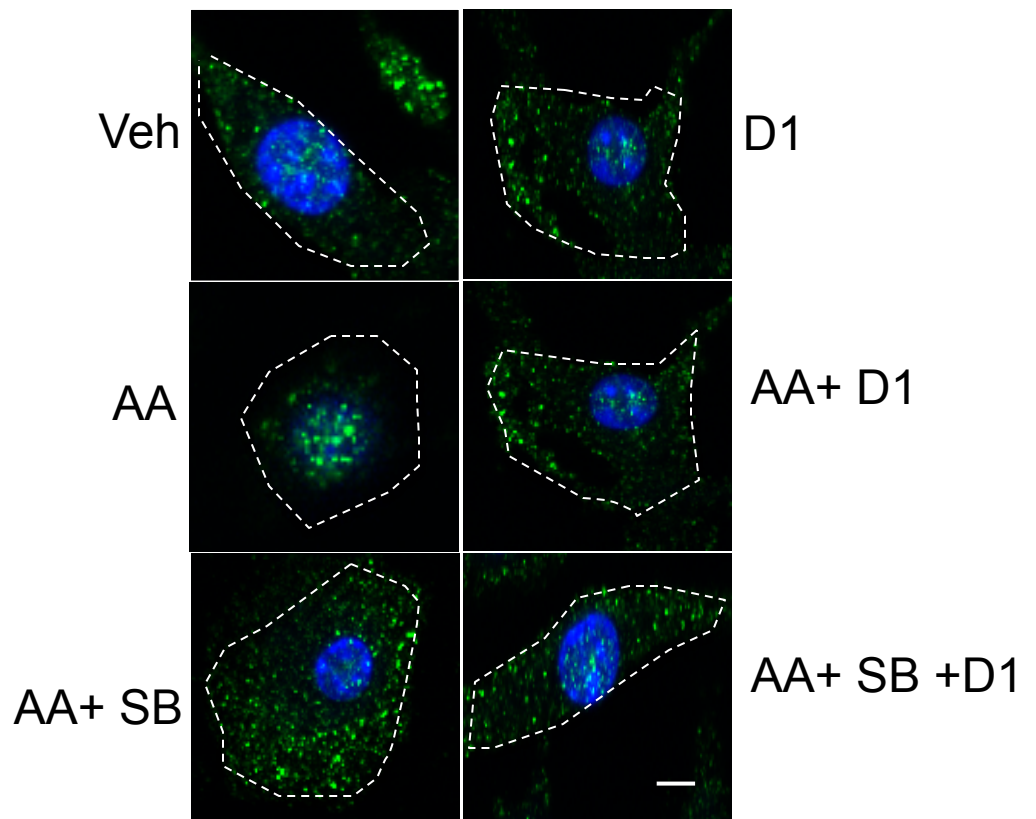


Fig. S5. RvD1 decreases nuclear localization of 5-LOX through inhibition of P38 signaling. Incubations were carried out as in Fig 2C. BMDMs were viewed by confocal microscopy at 40x magnification; the macrophages in each image is outlined (bar = 5 μ M). 5-LOX is green and the nuclear DAPI stain is blue.

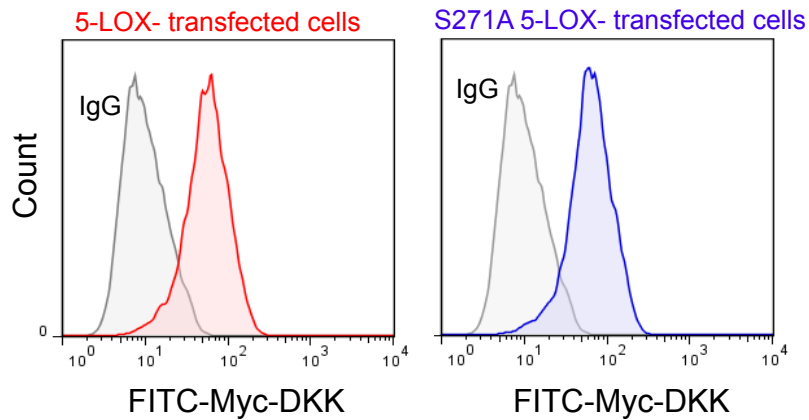


Fig. S6. Transfection of plasmids into macrophages. BMDMs were transfected with a complex of FLAG-tagged 5-LOX or S271A 5-LOX plasmids and Jet-Pei-Man reagent. After 72 h, the cells were subjected to flow cytometric analysis for anti-FLAG fluorescence. Representative flow cytometry histograms are shown.

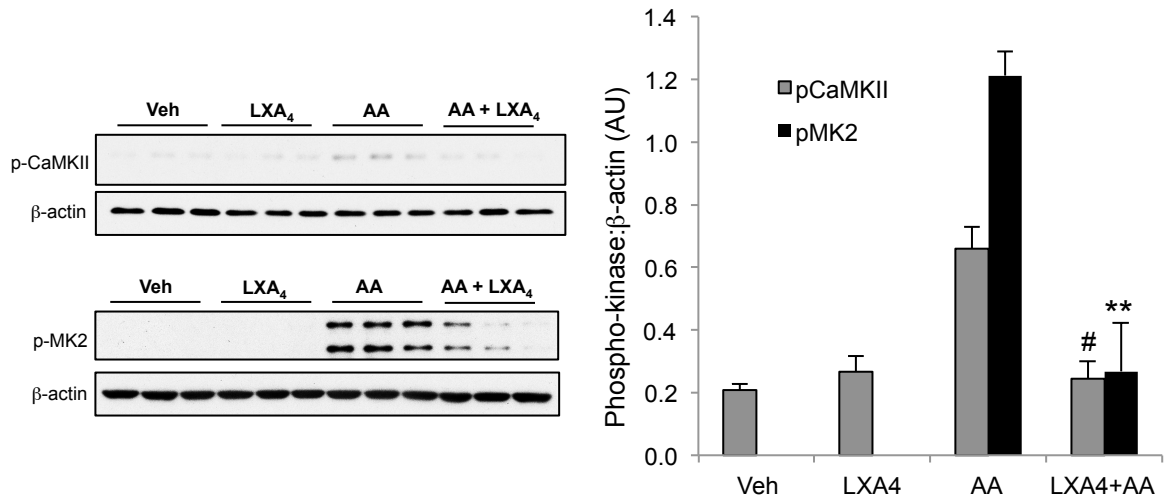


Fig. S7. LXA₄ suppresses activation of CaMKII and MK2 and decreases LTB₄ synthesis. (A) BMDMs were incubated with 1 nM LXA₄ or vehicle for 20 min at 37°C and then treated with 10 μM AA or vehicle for 5 min at 37°C. Cell lysates were subjected to immunoblotting for phospho-CaMKII and phospho-MK2 and quantified by densitometry ($n = 3$; mean \pm SEM; # $P < 0.001$ vs. AA).

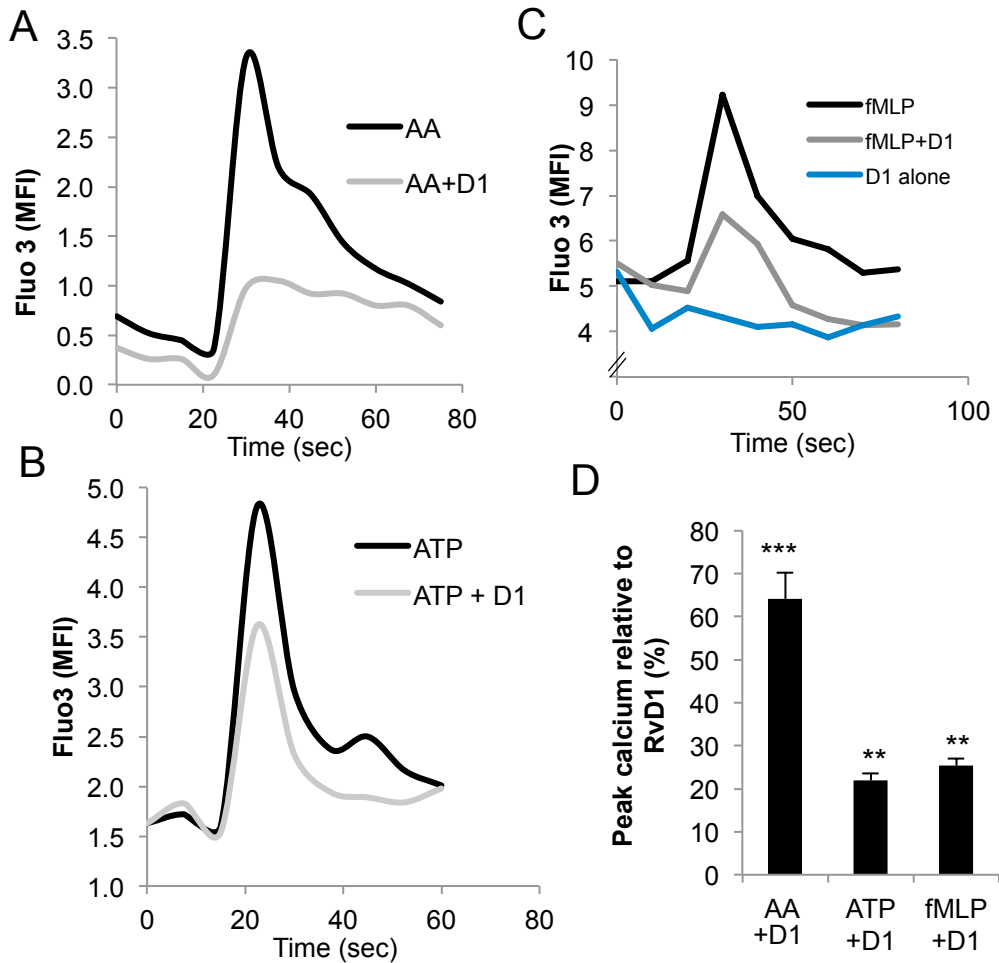


Fig. S8. RvD1 suppresses AA- or ATP-stimulated intracellular calcium increase. BMDMs were incubated with the calcium probe Fluo3 for 20 min in HBSS containing calcium, magnesium, 25 mM glucose, and 1:100 PowerLoad™, which helps solubilize the Fluo3 dye and contains probenidol for dye retention. Excess Fluo3 was removed, and BMDMs were then stimulated with 1 nM of RvD1 or vehicle control for another 20 min. 10 μ M AA (A), 10 μ M ATP (B) or 1 μ M fMLP (C) was added, and intracellular calcium was monitored by flow cytometry. (D) Percent peak intracellular calcium was quantified relative to RvD1 alone (n = 3, mean \pm SEM; ***P<0.0001, **P<0.01 vs. RvD1 alone).

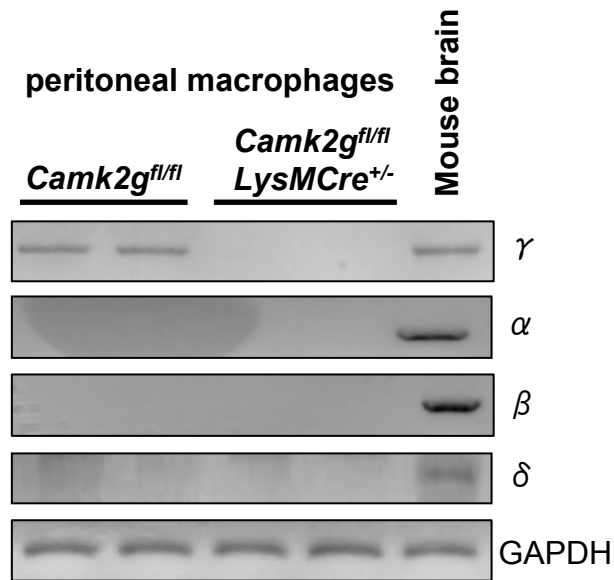


Fig. S9. CaMKII γ is the CaMKII isoform expressed in macrophages and is deleted in macrophages from *Camk2g^{fl/fl}LysMCre^{+/-}* mice. Peritoneal macrophages were harvested from *Camk2g^{fl/fl}LysMCre^{+/-}* and control *Camk2g^{fl/fl}* mice and assayed for the indicated isoforms of CaMKII by immunoblot. Mouse brain homogenate were used as a positive control for all four isoforms. GAPDH is the loading control.

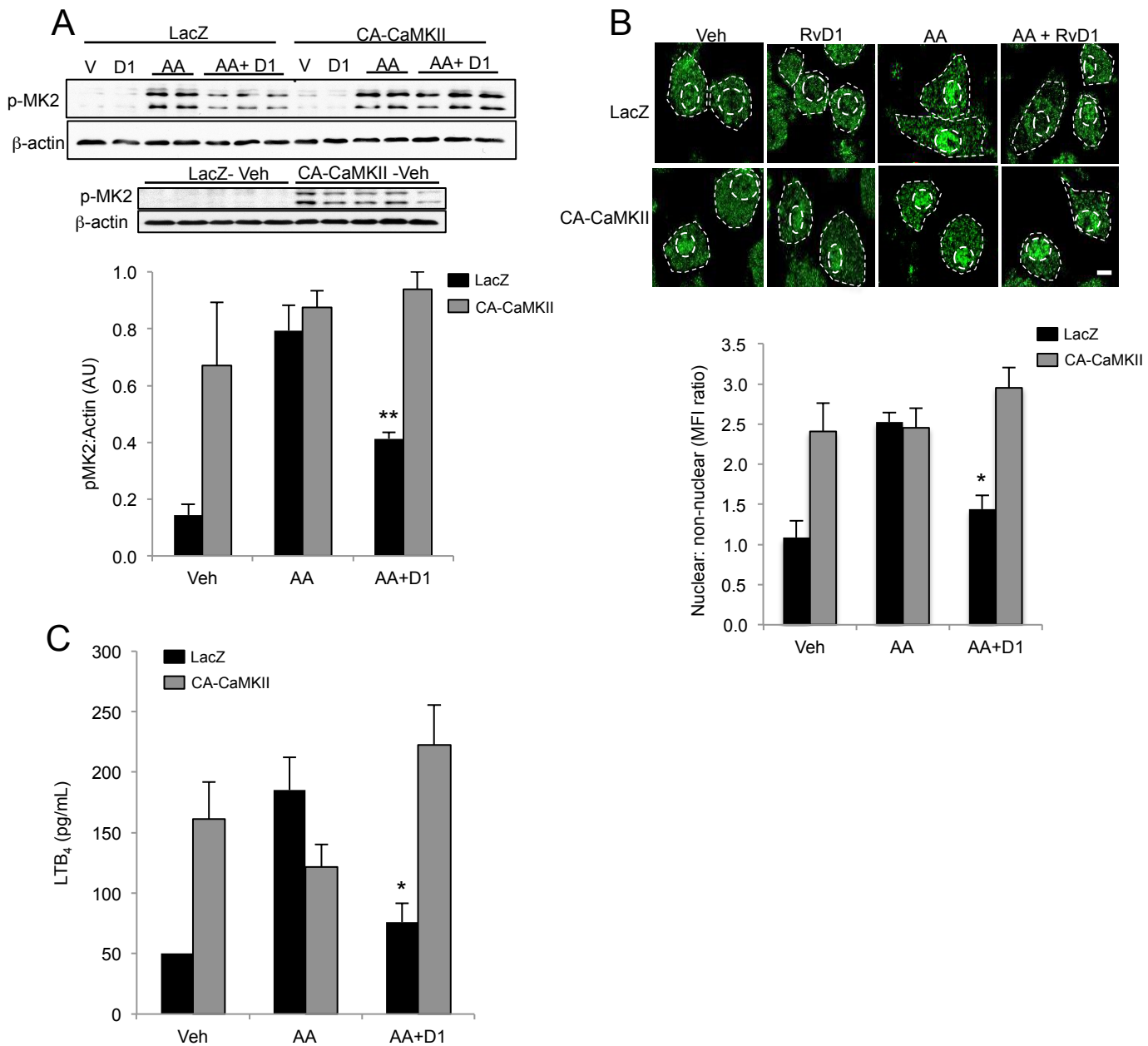


Fig. S10. The suppressive action of RvD1 on AA-stimulated p-MK2 is abrogated in macrophages overexpressing constitutively active CaMKII. BMDMs were transduced with LacZ or a constitutively active CAMKII (CA-CaMKII). After 72 h, the cells were treated as indicated. (A) Top blot is a representative p-MK2 immunoblot for all groups; because this blot only shows 1 Veh lane for each group, a blot with multiple Veh lanes is shown underneath. Densitometric ratio quantification is shown in the bar graph. (B) BMDMs were permeabilized and stained with Alexa-488 anti-5-LOX antibody (green) and counterstained with the nuclear stain DAPI (blue). Cells were viewed by confocal microscopy at 40x magnification; the macrophage in each image is outlined (bar = 10 μ m). Images were analyzed by ImageJ software for MFI of nuclear vs. non-nuclear 5-LOX staining in 5-7 cells per field. (C) LTB₄ was monitored by ELISA. For all bar graphs, $n = 3$ separate experiment; mean \pm SEM; ** $P < 0.01$ and * $P < 0.05$ vs. AA.

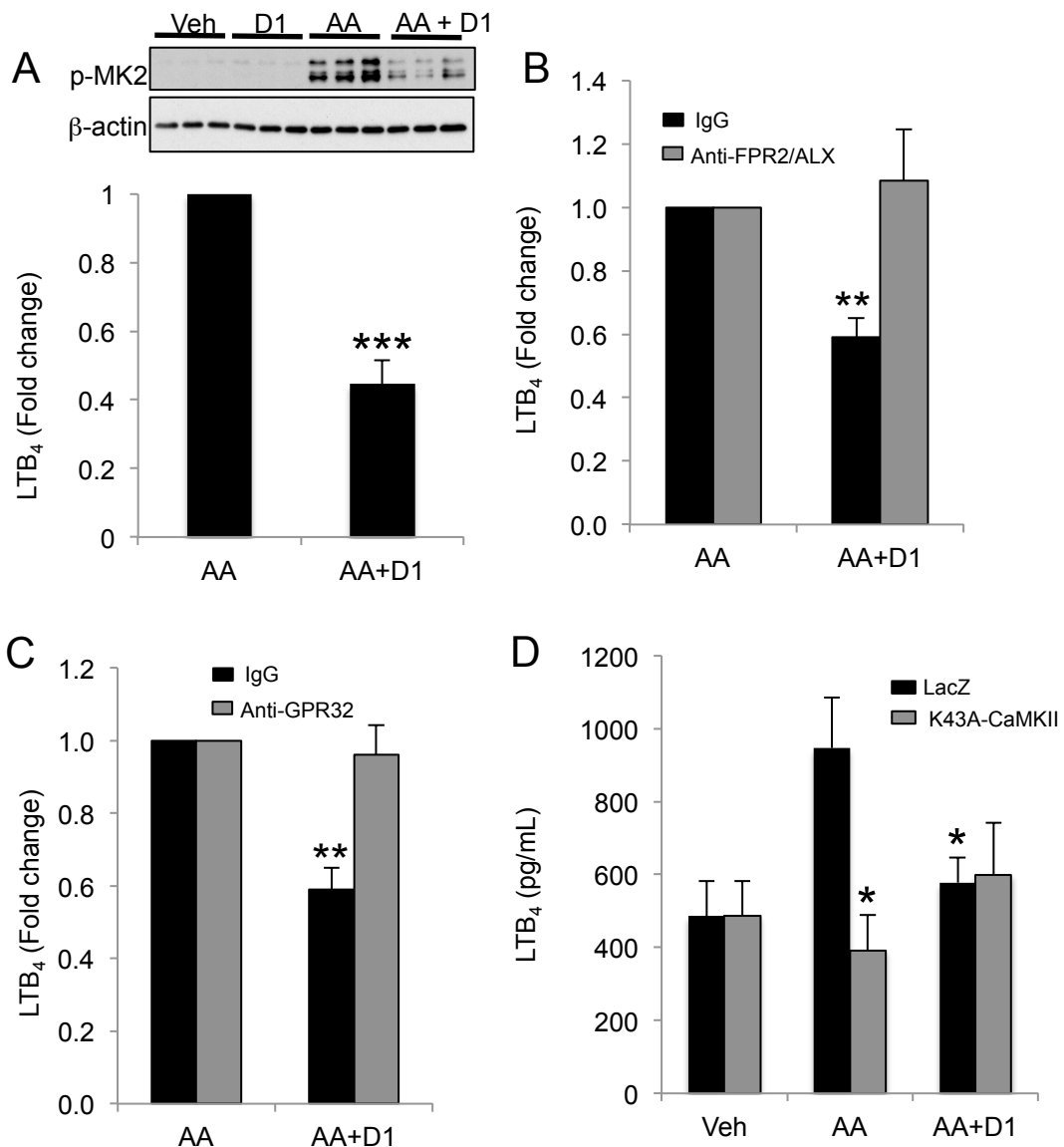


Fig. S11. RvD1 suppresses the CaMKII-MK2-LTB₄ pathway in human macrophages in a receptor dependent manner. (A) *Top panel*, Human monocyte-derived macrophages were incubated with 1 nM RvD1 or vehicle for 20 min at 37°C and then treated with 10 μ M AA or vehicle for 5 min at 37°C. Cell lysates were subjected to immunoblotting for phospho-MK2; the upper panel is a representative of 5 individual human donors, each analyzed in triplicate. *Bottom panel*, Incubations and LTB₄ ELISA were carried out as in Fig 1B ($n = 5$; mean \pm SEM; *** $P < 0.001$ vs. AA). (B,C) Incubations were carried out as above except that the cells were pre-treated with antibodies against the FPR2/ALX and GPR32 receptors ($n = 3$ mean \pm SEM; * $P < 0.05$ vs. all other groups). (D) Human macrophages were transduced with adenoviruses containing LacZ or dominant-negative K43A-CaMKII (each at 400 MOI) for 60 h and then incubated and assayed for LTB₄ as above ($n = 3$ mean \pm SEM; * $P < 0.05$ vs. AA).

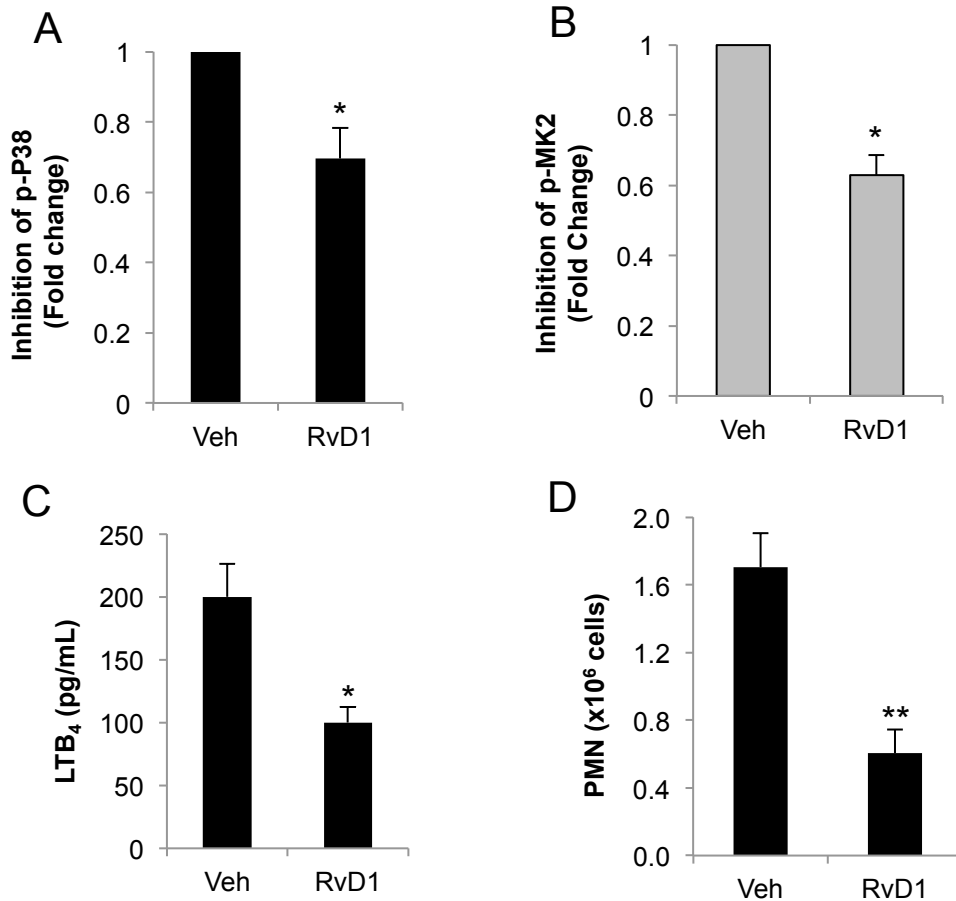


Fig. S12. RvD1 decreases macrophage p-MK2 and p-P38, LTB₄, and PMNs in zymosan peritonitis. Mice were injected i.v. with 10 ng RvD1 per mouse or vehicle control, and 15 min later 200 µg zymosan A per mouse was injected i.p. to induce peritonitis. Peritoneal lavages were obtained 2 h later. (A,B) Leukocytes were collected and assayed for p-P38 and p-MK2 by flow cytometry ($n = 3$, mean \pm SEM; * $P < 0.05$). (C,D) Exudates were assayed for LTB₄ and PMN numbers ($n = 4-5$ mice/group, mean \pm SEM; * $P < 0.05$ or ** $P < 0.01$).

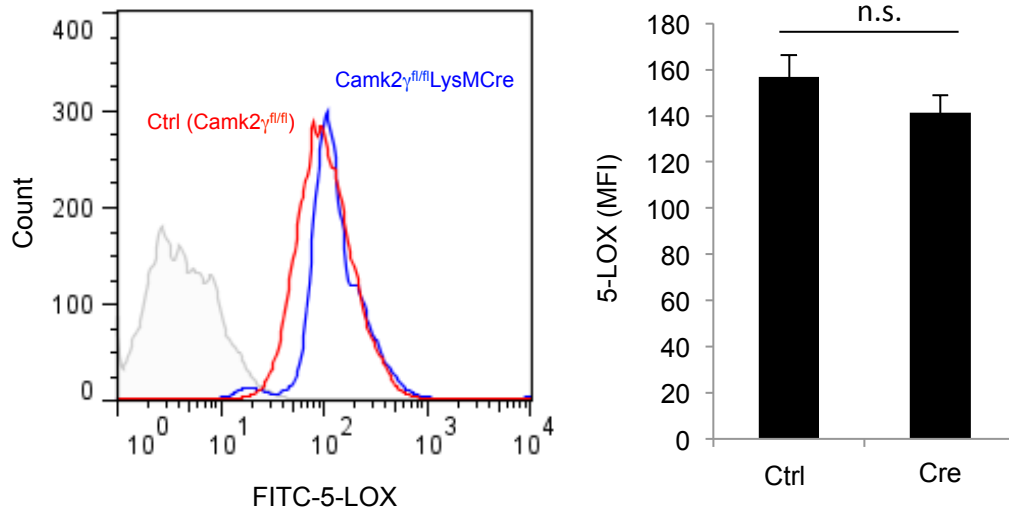


Fig. S13. 5-LOX protein levels are similar in CamK2 $\gamma^{fl/fl}$ and CamK2 $\gamma^{fl/fl}$ LysMCre $^{+/-}$ in zymosan-induced peritoneal exudate cells. Peritoneal exudate cells from zymosan-injected CamK2 $\gamma^{fl/fl}$ (Ctrl) and CamK2 $\gamma^{fl/fl}$ LysMCre $^{+/-}$ (Cre) mice were analyzed by flow cytometry for anti-5-LOX fluorescence. Representative flow cytometry histograms and quantification of FITC-5-LOX expression are displayed ($n = 3$ separate mice, mean \pm SEM; n.s., non-significant).

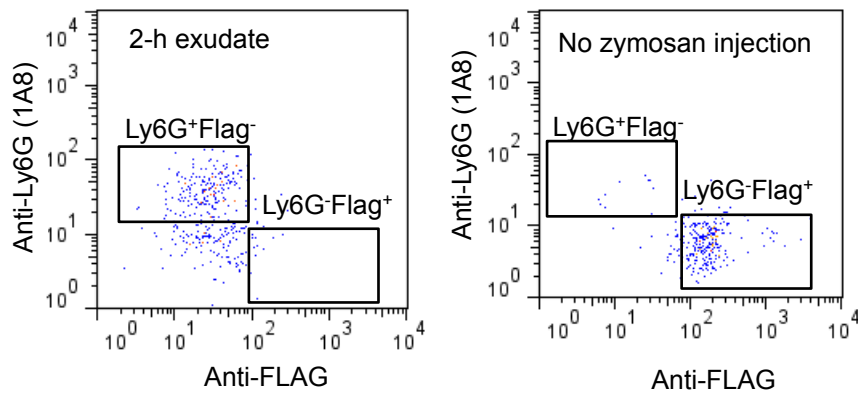


Fig. S14. In-vivo transfection is specific to macrophages. Mice were injected i.p. with a complex of FLAG-tagged *Alox5* plasmid and Jet-Pei-Man reagent. After 42 h, mice were injected i.p. with zymosan or vehicle control, and 2 h later, peritoneal cells were subjected to flow cytometric analysis for anti-FLAG fluorescence in PMNs (Ly6G⁺) and macrophages (Ly6G⁻). Representative flow cytometry histograms and dot plots are shown.

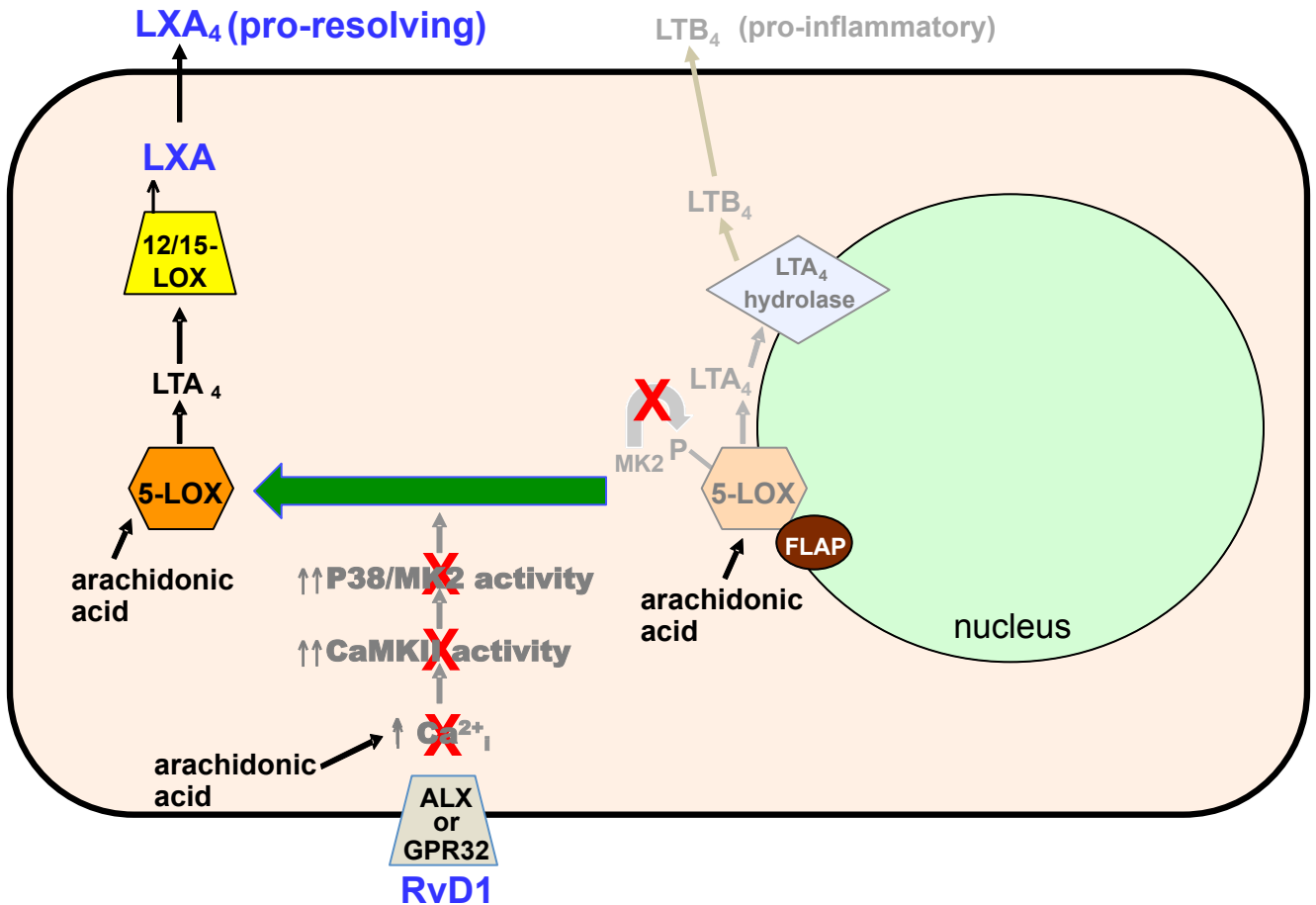


Fig. S15. Proposed scheme of RvD1-CaMKII-P38/MK2-LTB₄ pathway. RvD1, acting through the ALX or GPR32 receptor, decreases the increment in cytosolic calcium stimulated by AA, thereby decreasing activation of CaMKII. As a result, activation of the CaMKII-downstream kinases P38 and MK2 is suppressed, leading to decreased phosphorylation of 5-LOX. The decrease in p-5-LOX promotes its translocation from the nucleus to the cytoplasm, which leads to an decrease in LTB₄ and an increase in LXA₄. The scheme envisions the hypothesis, yet to be proven, that nuclear 5-LOX favors LTB₄ due to proximity to LTA₄ hydrolase, while cytoplasmic 5-LOX favors LXA₄ due to proximity to 12/15-LOX.

Supplemental Methods

Immunoblots. BMDMs (0.2×10^6 cells/well) were plated in 24-well plates and placed in media containing 0.05% FBS. After 12 h, the media were removed, and the cells were incubated at 37°C in serum-free media containing either vehicle control or 1 nM RvD1 for 20 min, followed by incubation with 10 μ M AA for 5 min. After removal of the media, the cells were flash-froze in liquid nitrogen. Extracts prepared from the frozen cells were electrophoresed on 4–20% gradient SDS-polyacrylamide gels and transferred to 0.45- μ m nitrocellulose membranes. The membranes were blocked at room temperature for 1 h in Tris-buffered saline containing 0.1% Tween 20 (TBST) and 5% (w/v) BSA and then incubated sequentially with primary antibody in TBST/BSA at 4°C overnight and secondary antibody coupled to horseradish peroxidase. Proteins were detected by ECL Supersignal West Pico chemiluminescence (Pierce).

Zymosan A-stimulated peritonitis. Six-eight wk/o female mice were administered 10 ng RvD1 per mouse by i.v. injection. After 15 min, 200 μ g zymosan A per mouse was injected i.p. to induce peritonitis as in (1). After 2 h, peritoneal exudates were collected by a lavage with 2.5 mL cold PBS. Exudate cells were quantified using trypan blue exclusion, and differential cell counts were assessed via flow cytometry using a FACS Canto flow cytometer. For these analyses, cells were stained with FITC-conjugated rat anti-mouse Ly-6G (clone 1A8), PE-conjugated F4/80, or rat IgG2c, κ isotype control. In parallel, cells were permeabilized and assayed for intracellular kinase activity, and peritoneal

exudate supernatants were subjected to LTB₄ ELISA analysis. All procedures were conducted in accordance with protocols approved by the Columbia University Standing Committee on Animals guidelines for animal care (Protocol # AC-AAAF7107).

Mice lacking macrophage CaMKII γ . *Camk2g*^{fl/fl} mice were generated by flanking exon 1-2 with *loxP* sites and then crossed onto the C57BL/6J background. *LysMCre*^{+/-} mice were generated as described previously (2, 3). *Camk2g*^{fl/fl} and *LysMCre*^{+/-} mice were crossed to generate the macrophage-CaMKII γ -deficient mice used for this study.

Identification and quantification of eicosanoids by LC-MS/MS. Inflammatory exudates or activated BMDMs were collected and combined with 2 volumes of cold (4°C) methanol. Samples were immediately frozen at -80°C to allow for protein precipitation. After addition of internal deuterium-labeled standards (d4-LTB₄, d8-5-HETE, d4-PGE₂; Cayman Chemical), lipid mediators were extracted using solid-phase C18 columns. Butylated hydroxytoluene was added prior to extraction to prevent non-enzymatic oxidation of lipids during sample preparation. Methyl formate fractions were taken to dryness under N₂ gas and suspended in methanol for LC-MS/MS analysis. Lipid mediators of interest were profiled using an HPLC system (Shimadzu Prominence) equipped with a reverse-phase (C18) column (4.6mm x 50mm; 5.0 μ m particle size) coupled to a triple quadrupole mass spectrometer (AB Sciex API2000), which was operated in negative

ionization mode. The mobile phase consisted of water:acetic acid (100:0.1 v/v) and acetonitrile:methanol (4:1 v/v) at a ratio of 73:27, which was ramped to 30:70 over 11 minutes and to 20:80 over the next 10 min. After holding for 2 min, the mobile phase was ramped to 0:100 for 2 min before returning to 73:27. The flow rate was held constant at 300 μ L/min. Multiple reaction monitoring (MRM) was used to identify and quantify LTB₄ (335>195), 6-*trans*-LTB₄ (335>195), 20-hydroxy LTB₄ (351>195), 5-HETE (319>115), 12-HETE (319>179) and LXA₄ (351>115) (4). Quantification of lipid mediators was performed using external calibration curves for each mediator based on authentic standards (Cayman Chemical) and was normalized to recovery of internal deuterium-labeled standards (see above).

1. Norling LV, Dalli J, Flower RJ, Serhan CN, & Perretti M (2012) Resolvin D1 Limits Polymorphonuclear Leukocytes Recruitment to Inflammatory Loci: Receptor-Dependent Actions. *Arterioscler Thromb Vasc Biol.*
2. Clausen BE, Burkhardt C, Reith W, Renkawitz R, & Forster I (1999) Conditional gene targeting in macrophages and granulocytes using LysMcre mice. *Transgenic Res* 8(4):265-277.
3. Ozcan L, *et al.* (2013) Activation of Calcium/Calmodulin-Dependent Protein Kinase II in Obesity Mediates Suppression of Hepatic Insulin Signaling. *Cell Metab* 18(6):803-815.
4. Yang R, Chiang N, Oh SF, & Serhan CN (2011) Metabolomics-lipidomics of eicosanoids and docosanoids generated by phagocytes. *Curr Protoc Immunol* Chapter 14:Unit 14 26.